ORIGINAL ARTICLE

Design of *Vitex Negundo* Nanoemulsion for Anti-Inflammatory Activity Targeting Anal Fissure

Chanchal Chaurasiya[1,2], Jitendra Gupta[2]

[1]*Department of Pharmaceutics, NKBR College of Pharmacy and Research Centre, Meerut, Uttar Pradesh, India,*
[2]*Department of Pharmaceutics, Institute of Pharmaceutical Research, GLA University, Mathura, Uttar Pradesh, India*

Abstract

Aim: The aim of this study was to design and characterize a topical nanoemulsion of *Nirgundi* oil for the treatment of anal fissures and to evaluate its *in-vitro* anti-inflammatory activity and *in-vivo* anal fissure healing potential. **Materials and Methods:** A pseudo-ternary phase diagram was constructed to determine the Northeast region suitable for nanoemulsion formation. Based on this, six different batches of nanoemulsion were prepared. These formulations were characterized for globule size and surface morphology, refractive index, zeta potential, pH, viscosity, drug-excipient compatibility, drug entrapment and loading efficiency, thermodynamic stability, and *in-vitro* drug permeation. From the six batches, B6 was selected as the best formulation and subjected to further in-vitro anti-inflammatory testing using the egg albumin denaturation and COX-II enzyme inhibition assay. Additionally, in-vivo anal fissure healing activity was assessed using histological analysis of tissue samples. **Results and Discussion:** The B6 formulation demonstrated significant *in-vitro* anti-inflammatory activity, with 91.17% suppression in the egg albumin denaturation assay compared to 79.38% for the reference drug (diclofenac). The COX-II inhibition assay revealed an IC_{50} of 3.735 µg/mL for B6, which was more effective than the marker sabinene (IC_{50}: 6.594 µg/mL). *In-vivo* studies confirmed that the B6 formulation showed significant improvement and healing of anal fissures, indicating successful therapeutic action. These results suggest that the nanoemulsion enhances the bioavailability and therapeutic efficacy of *Nirgundi* oil for local treatment. **Conclusion:** The study finally concluded that the topical nanoemulsion formulation of *Nirgundi* oil (B6) has potent anti-inflammatory action and effectively promotes healing in anal fissures. It showed significant therapeutic potential and can be considered a promising candidate for further development as a topical treatment for anal fissures.

Key words: Cox-II enzyme inhibition, egg albumin denaturation, nanoemulsion, nirgundi oil, sabinine

INTRODUCTION

A longitudinal split in the distal anoderm's squamous epithelium is referred to as an anal fissure. It usually shows up in the rear midline. Anal fissures possess two different types: Acute and chronic. Even though an acute anal fissure can cause painful defecation and rectal bleeding, it usually heals in 1–2 weeks with conservative treatment and dietary changes. Conversely, a chronic anal fissure lasts longer than 4–6 weeks. This kind of anal fissure is thought to be a very common and excruciating perianal ailment that is resistant to conservative treatment.[1,2] The internal anal sphincter hypertonia observed in patients with anal fissures has long been believed to be a secondary phenomenon, occurring after local trauma to the mucosa, such as the passage of hard feces, even though the exact cause of anal fissure remains unknown.[3]

Oral pain relievers, stool softeners, regional anesthesia, high-fiber dietary regimens, plenty of drinks, and a warm sitz are typical conservative treatments for anal fissures.[4] Surgical intervention is implemented when conservative treatment is ineffective. The most common technique for treating anal fissures has been surgery for centuries, involving anal dilatation, lateral internal sphincterotomy, and posterior midline sphincterotomy, which leads to post-operative incontinence with surgical therapy. Anal fissure recurrence

Address for correspondence:
Dr. Jitendra Gupta, Institute of Pharmaceutical Research, GLA University, Chaumuhan, District-Mathura - 281 006, Uttar Pradesh, India.
Phone: +91-8979136611.
E-mail: smartjitu79@gmail.com; jitendra.gupta@gla.ac.in

Received: 04-02-2025
Revised: 19-03-2025
Accepted: 28-03-2025

is another potential issue that may arise shortly after surgery.[5-7] Conservative management is unlikely to resolve fissures caused by underlying diseases, such as perianal Crohn's disease, where the fissures are frequently multiple and lateral. Botulinum toxin injection is a potent treatment for anal fissures, but it is invasive, painful, and costly. Glyceryl trinitrate topical treatment experienced difficulties with headaches and low blood pressure. The main benefits of topical medication therapies include increased patient compliance, potentiated efficacy, decreased side effects, and lower costs.[8]

Multiple unani drugs are indicated to treat anal fissures that possess properties of Mudammil-e-qurooh (Healing), Muhallil-e–awraam (Anti-inflammatory), and Muzalliq (Lubricant). In this book, Kitab-ul-Hawi, Zakariya Razi stated that topical application is highly advantageous for treating anorectal fissures.[9] Medicinal plant products and nutritional therapies are an essential part of safe and efficient hemorrhoid treatment when compared to surgical and non-surgical procedures. It has been shown that herbal medicines improve capillary flow, connective tissue strength, perivascular amorphous substrate microcirculation, and vascular tone.[10] Based on their indigenous knowledge, people from many different tribes and cultures have treated hemorrhoids with a variety of ethnomedicinal plants.[11,12]

Vitex negundo L. is a shrub or small tree that grows in many tropical, subtropical, warm, and even temperate regions of the world. The names Nirgundi and five-leaved chaste tree also know it. It can grow to 1500 m in almost every region of India.[13] Several traditional medical systems have historically employed the plant for therapeutic purposes. It is also recognized to have many biological qualities, including nematicidal, insecticidal, antitumor, antimicrobial, antiseptic, anti-inflammatory, and antitumor effects.[14-16] Nirgundi helps manage anal complications due to its vata balancing and kashaya (astringent) properties. It helps prevent constipation and reduces the symptoms of inflammation and bleeding, thereby providing relief.[17]

The low membrane permeability of the plant bioactive compounds resulting from their large molecular size also limited their therapeutic uses. By enhancing the solubility and absorption profile of herbal bioactives, as well as reducing dosage and adverse effects, nanocarriers can maximize their effectiveness. The herbal bioactives can be directed by the nanoemulsions to a specific target site and kept at a higher concentration in the bloodstream for extended periods. However, these particular requirements were not met by the traditional drug delivery system. The solubility, shelf life, permeation, and bioavailability of the herbal bioactives may all be enhanced by nanoemulsions.[18] Transparent or translucent emulsions with droplet sizes between 20 and 500 nm are known as nanoemulsions. The physicochemical properties and droplet characteristics determine the stability and application of nanoemulsions. The parameters that are used to investigate the droplet properties are the size, composition, concentration, zeta potential, polydispersity, and interfacial tension. The physicochemical qualities are examined in terms of optical, rheological, gravitational, droplet aggregation, Ostwald ripening, and chemical stability.[19,20]

MATERIALS AND METHODS

Materials

Nirgundi oil was procured as a free sample from Shayona Aromatics (Mumbai, Maharashtra, India). Tween-80 and Span-20 were bought from CDH (Delhi, India). The other reagents and chemicals are of AR class.

Methods

Construction of pseudoternary phase diagram

To create nanoemulsion systems with the required physicochemical properties, it is essential to choose the right concentration of each component. The development of traditional pseudo-ternary phase diagrams has been investigated as a means of improving multi-component emulsion formulation.[21] The ternary phase diagrams were created using the aqueous titration technique.[22] A number of systems with varying concentrations of surfactant and oil (drug): Mixture of co-surfactants (Smix).[23,24] The component systems are shown in Table 1.

Each system had distilled water added to it until turbidity was produced, and the volume of water needed to do so was noted. The percentage w/w of each system component was determined using the following formulas: [25-27]

$$\text{wt}\,\%\,\text{of A} = \frac{\text{A}}{\text{D}} \times 100 \quad (1)$$

Table 1: Component system for the development of phase diagram

Nirgundi oil (Drug) (mL) (A)	Surfactant (Tween 80+SPAN 20) (mL) (B)
1	4.5+4.5
2	4.0+4.0
3	3.5+3.5
4	3.0+3.0
5	2.5+2.5
6	2.0+2.0
7	1.5+1.5
8	1.0+1.0
9	0.5+0.5

$$\text{wt}\,\%\,\text{of B} = \frac{B}{D} \times 100 \quad (2)$$

$$\text{wt}\,\%\,\text{of C} = \frac{C}{D} \times 100 \quad (3)$$

Where; A = Nirgundi oil (Drug), B = S_{mix} (Tween 80 + Span 20), C = Water, D = Weight of mixture.

Formulation and preparation of nanoemulsions

According to prepared ternary phase diagrams, six batches of North East (NEs) of nirgundi oil were prepared using ultrasonication[28-30] (PCI, NKBR, Meerut).

Characterization of prepared nanoemulsions

Determination of globule size and surface morphology

Globule size and surface morphology of prepared batches of nanoemulsions were evaluated by FESEM[31,32] (Hitachi-PU 10.0 kV), from SAIF PU.

Refractive index measurement

The refractive index is a crucial metric for assessing an objective's ability to gather light and resolve. A refractive index of 1.32 for the nanoemulsion suggested that the medication was isotropic.[33] The refractive index of the prepared nanoemulsion were evaluated using a Digital Abbe Refractometer (Milwaukee, MA871).

Zeta potential measurement

Another significant factor that directly impacts the stability of nanoemulsions is zeta potential. Higher charge levels cause reduced droplet coalescence.[34,35] The prepared nanoemulsion's zeta potential was evaluated using Malvern Zetasizer (Version 8.00.4813), which was done at AIIMS, New Delhi.

pH measurement

The rectum has a neutral pH of 7–8 and an average fluid content of 1–3 mL, with little buffering capability.[36] Variations in the pH of the formulation may irritate the site of administration. Using a digital pH meter, the produced nanoemulsion's pH was measured (Electronics India, NKBR, Meerut).[37]

Viscosity measurement

Viscosity is an important parameter for nanoemulsions. Elevated viscosity exhibits a lessened transmembrane flow and smaller oil droplets due to raising the membrane pores' internal wall shear stress.[38] A Brookfield viscometer (LV-DVE) was used to measure the prepared nanoemulsion formulation's viscosity.

Preparation of calibration curve

Calibration curves are utilized to quantitatively analyze an unknown and comprehend the instrumental response to an analyte.[39] Multiple dilutions of the formulation were prepared using concentrations 2, 4, 6, 8, 10, and 12 µg/mL. The absorbance of each dilution was measured at 230 nm wavelength. A plot of absorbance versus concentration for the measured values was created.

Fourier transform infrared spectroscopy (FTIR): Drug excipient compatibility study

For the purpose of determining modifications to drug-excipient mixtures, FTIR is a practical technology. The presence of interactions between the API and the excipient under investigation is indicated by the formation of new peaks, the loss of an absorption peak, or a decrease in peak strength.[40] The drug-excipient compatibility of nanoemulsion formulation was evaluated using FTIR (IR Affinity, Japan).

Drug entrapment efficiency and drug loading efficiency (DEE and DLE)

The amount of drug that is entrapped into nanoparticles and the proportion of the weight of the nanoparticle that is composed of the drug are assessed using DEE and DLE, respectively.[41,42] The weight amount of the formulation was dispersed in ethanol by ultra-sonication. The drug content was estimated spectroscopically using 230 nm after making a 1000 ppm solution. The eq. (4) and eq. (5)[41] were used to calculate the entrapment efficiency and loading efficiency.

$$\text{Drug EE} = \frac{\text{Drug content in the product obtained (mg)}}{\text{Total ammount of drug added (mg)}} \times 100 \quad (4)$$

$$\text{Drug LE} = \frac{\text{Drug content in the product obtained (mg)}}{\text{Total product wt (mg)}} \times 100 \quad (5)$$

Thermodynamic stability study

The nanoemulsion has a longer shelf life due to thermodynamic stability in comparison to regular emulsions. It sets them apart from emulsions and will eventually phase separate and have kinetic stability. Thermodynamically stable formulations were chosen for additional research.[43,44] Six heating-cooling cycles were performed to ascertain if NEs are thermodynamically stable. The temperature was set between 4° and 45°C and store the NEs at each temperature for 48 h. For the NEs formulations that are stable at 4°C and 45°C, phase separation was monitored during a 30-min centrifugation at 3500 rpm.

In vitro drug permeation study

The *in vitro* permeation studies were used to demonstrate that nanoemulsions could increase topical drug delivery when compared with the other routes.[45] This study was done with the help of cellophane membrane through Franz diffusion cell which was having 0.75 cm^2 diameter and volume capacity of 25 mL. Phosphate buffer (25 mL) pH 7.4 is filled in the receptor compartment and cellophane membrane was placed in between receptor and donor compartment. 5 mL of NEs was filled in donor compartment. The entire assembly

was set up on a magnetic stirrer, and a magnetic bead was used to stir the solution in the receptor compartment at 50 revolutions/min. The temperature was set to 37° ± 0.5°C at specific time intervals (5, 10, 15, 20, 25, 30, 45, 60, 90, 120, 180, and 240 min); 2 mL of sample was withdrawn and examined for drug with the help ultraviolet spectrophotometer at 230 nm.[46,47]

Selection of best formulation

All the batches of prepared nanoemulsion were evaluated successfully to optimize the best formulation on the basis of all the parameters that satisfy and pass the criteria of good nanoemulsion formulation.

In vitro anti-inflammatory activity

The best-selected nanoemulsion formulation undergoes *in vitro* anti-inflammatory activity. The produced nanoemulsion's anti-inflammatory properties are detected using two techniques:

- Egg albumin denaturation method
- Cox II enzyme inhibition method

Egg albumin denaturation method

The basic idea behind the egg albumin denaturation assay is that anti-inflammatory medications could preserve protein structures and prevent denaturation, which is frequently linked to inflammation and tissue damage. The solutions listed below need to be made before the egg albumin test.

Preparation of 1% of egg albumin solution: A solution of egg albumin was prepared using a fresh hen's egg. The egg was cracked carefully, and 1 mL of the translucent portion was transferred to 100 mL of distilled water, thoroughly stirring.

Preparation of diclofenac solution (reference solution): We weighed accurately about 5 mg diclofenac and solubilized in 5 mL distilled water.

Preparation of test solution: The test solution was prepared by dissolving 2 mL of the nanoemulsion formulation in 2.8 mL of phosphate buffer (pH 7.4).

Preparation of control solution: Control solution was prepared by dissolving 2 mL distilled water in 2.8 mL phosphate buffer (pH 7.4).

Egg albumin assay: The method for the egg albumin assay is given hereunder in Table 2:[47-51]

The following formula was used to determine the percentage of protein denaturation inhibition:

$$\text{Percentage inhibition} = \frac{\text{Absorbance of control} - \text{Absorbance of test sample}}{\text{Absorbance of control}} \times 100 \quad (6)$$

Cox II enzyme inhibition method: The bioconversion of arachidonic acid to inflammatory prostaglandins (PGs) is mediated by the enzyme cyclooxygenase (COX), which is competitively inhibited by some medicines.[52-55] A group of lipid molecules known to mediate both acute and chronic inflammation are PGs.[56,57] Various assay methods were reviewed for the assessment of *in vitro* COX activity and mode of inhibition by sample compounds.[58,59] The *in vitro* Cox II enzyme inhibition study was done by Aakar Biotech, Lucknow.

Reagents and buffers

Extract dilutions: Prepare dilutions from 0 to 500 µg/mL in Tris Cl buffer, pH 8.0.

Arachidonic acid, 10 mM (Substrate): Create a 10 mM stock solution (3.06 mg/mL) of arachidonic acid and sodium salt (Nu-Chek-Prep), using water, and freeze 0.5-mL aliquots for several months at −20°C. Dilute to 1 mM to be used as a working solution.

COX enzyme solution, 2 mg/mL: Dissolve the COX enzyme, ideally in a purified form (e.g., Cayman), at a concentration of 2 mg/mL in tris-buffered saline containing 3-[(3-cholamidopropyl)

Table 2: Method for egg albumin assay

Test solutions	Reference solution	Control solution
0.2 mL, 1% solution of egg albumin+2 mL formulated nanoemulsion+2.8 mL phosphate buffer ↓ For half an hour, incubate at 37±2ºC ↓ Heated for 15 min on water bath at 70±2ºC ↓ Measure absorbance using UV spectroscopy at 280 nm	0.2 mL, 1% solution of egg albumin+2 mL diclofenac solution+2.8 mL phosphate buffer ↓ For half an hour, incubate at 37±2ºC ↓ Heated for 15 min on water bath at 70±2ºC ↓ Measure absorbance using UV spectroscopy at 280 nm	0.2 mL, 1% solution of egg albumin+2 mL distilled water+2.8 mL phosphate buffer ↓ For half an hour, incubate at 37±2ºC ↓ Heated for 15 min on water bath at 70±2ºC ↓ Measure absorbance using UV spectroscopy at 280 nm

dimethylammonio]-1-propanesulfonate (CHAPS) (100 mM Tris·Cl, pH 7.5, 0.9% NaCl, and 0.4% (w/v) CHAPS). Freeze 1-mL aliquots at −80°C (they can remain stable for several years). Dilute to 100 U/mL to be used as working solution.

N,N,N', N'-Tetramethyl-p-phenylenediamine (TMPD), 17 mM: Create a 17 mM stock solution (4 mg/mL) of TMPD (from Sigma) using H_2O and keep 0.5-mL aliquots in storage at –20°C. Dilute to 2 mM to be used as working solution.

Colexib, 17 mM (Positive control): Prepare a 50 mM stock of dimethyl sulfoxide (DMSO) and store 0.5-mL aliquots at −20°C. Dilute to 500 µM to be used as working solution.

Tris/heme/phenol buffer, composition for 4 mL: 400 µL 1 M Tris·Cl, pH 8.1 (100 mM final) 4 µL 100% water-saturated phenol, 1 mM (1 µM final conc.) 40 µL bovine hemin chloride in DMSO, 100 µM (1 µM heme final conc.)

Procedure

Sample dilutions ranging from 0 to 500 µg/mL were made in Tris Cl buffer at pH 8.0. Each well of a 96-well plate was filled with the reaction components as outlined in the reaction mixture set-up table. The reaction commenced with the addition of 5 µL of substrate and 5 µL of TMPD solution, followed by a 10-min incubation period at room temperature. A microplate reader (iMark, BioRad) was then used to analyze the absorbance at 595 nm. Table 3 shows the composition of the reaction mixture.

In vivo anal fissure healing activity

Anal fissure invasion, grouping of animals, and anal fissure healing activity

A nichrome wire (24 SWG) was used to produce atrial fibrillation (AF) as part of a modified and standardized physical damage procedure. We disinfected the nichrome wires with alcohol. The rectum was then torn linearly using a 100 g weight suspended on the wire.

Two groups of six male Wistar rats, each weighing 150–200 g, were allocated at random. Rats that had fasted overnight were utilized for AF induction, and they were anesthetized with a solution of 1.0 mL 5% ketamine and 1.0 mL 2% xylazine. 24 SWG of nicrome wire was strung with a 100 g weight to cause AF. A linear rip, slit, or abrasion was made by inserting the wire's pointed end into the anal region, softly compressing it, and then pulling it back. Since only the anal region could be reached by the distance, the AF induction is restricted to the anorectal region. An obvious indication of the induction was the appearance of a bloodspot in the anal region. Every rat underwent this procedure, with each group receiving the same weight and pressure.

Each group contained six rats. Group 2 tested 1 (treated with a marker (sabinine) incorporating nanoemulsion sample), Group 3 was test 2 (treated with prepared formulation), and Group 1 was the normal (no induction). After the 5th day, the study animals received a 0.2 mL sample through the rectal region, and their body weights were recorded every day for 7 days. All the animals were put to sleep on the final day of the study by cervical dislocation; the rectum was then removed, examined closely for any visible textural changes, and preserved in formalin for additional histological analysis. To assess AF in clinical settings, the anorectal sections were histopathologically inspected for any alterations.

Histopathological examination

Rats' anal portions of their rectal tissues were preserved in immersed in paraffin with 10% formalin and divided into 3–5 µm thick pieces. For histological examination, an Olympus light microscope was used to view sliced pieces after they had been stained with hematoxylin eosin.

RESULTS AND DISCUSSION

Construction of pseudo-ternary phase diagram

The ternary phase diagram was plotted (TernaryPlot.com) based on the found concentration of each component calculated, as shown in Table 4 and the miscible and immiscible regions were marked as shown in Figure 1.

- In the ternary phase diagram: A = Drug (Nirgundi Oil); B = Surfactant (Tween −80 + SPAN 20); C = Water
- As per the ternary phase diagram, the concentration of the elements is A = 9.26–76.66%; B = 11.94–71.41%; C = 12.01–23.74%.

Table 3: Reaction mixture composition

Groups	Buffer	Sample	Inhibitor	COXII	THP buffer	Substrate	TMPD
Group 1	5 µL	-	-	10	80	5	5
Group 2	10 µL	-	-	10	80	-	5
Group 3	-	5	-	10	80	5	5
Group 4	5 µL	5	-	10	80	-	5
Group 5	-	-	5	10	80	5	5
Group 6	5	-	5	10	80	-	5

Formulation and preparation of nanoemulsions

On behalf of the ternary phase diagram, six batches of nanoemulsion were prepared, as given in Table 5, using the ultra-sonication method (PCI, NKBR, Meerut).

Characterization of prepared batches of nanoemulsions

Determination of globule size and surface morphology

Every formulated batch was obtained in the globule size range of 52.5–143.5 nm with a similar size distribution. The mean globule of the formulation is better positioned to the definition of the nanoemulsion (50–200 nm) along with the best polydispersity index, which indicates the similarity of droplet size, shown in Table 6 and Figure 2.

Refractive index measurement

The results of the refractive index study represent the isotropic nature of the drug. The outcomes are shown in Table 6.

Table 4: Concentration of each component

Nirgundi oil (mL) (A)	S_{mix} (mL) (B)	Water (mL) (C)
9.26	71.41	19.32
14.67	61.67	23.74
21.75	62.1	16.05
28.8	55.12	16.06
37.49	47.75	14.75
45.12	36.45	18.41
51.68	32.94	15.37
61.14	21.17	16.67
76.66	11.94	12.1

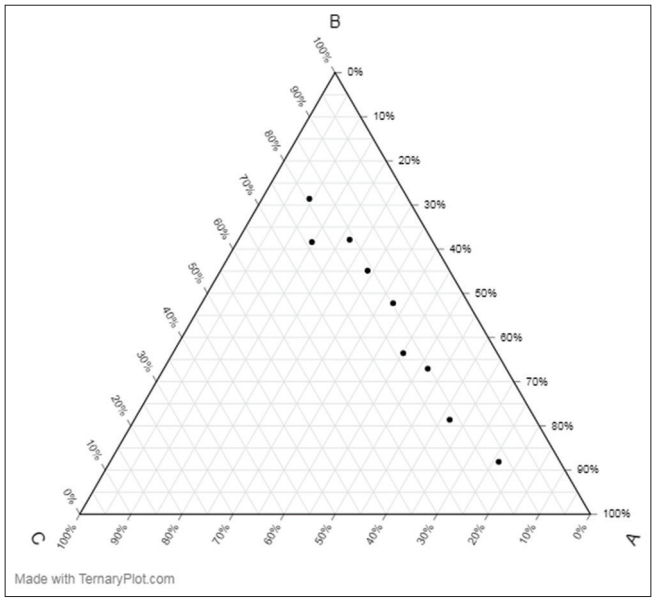

Figure 1: Phase diagram for nanoemulsion formulation

Zeta potential measurement

Table 6 and Figure 3 show the findings of the zeta potential, which represents mutual repulsion between the globules and assures the stability of the nanoemulsion formulation.

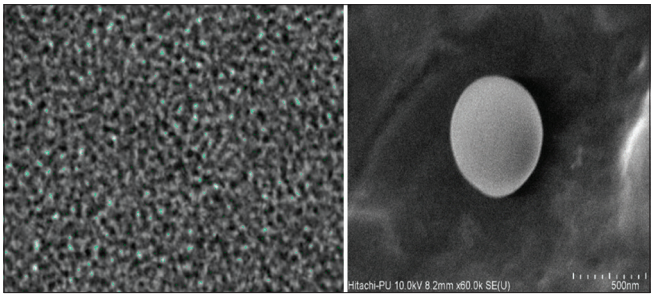

Figure 2: Scanning electron microscopy images of prepared nanoemulsion

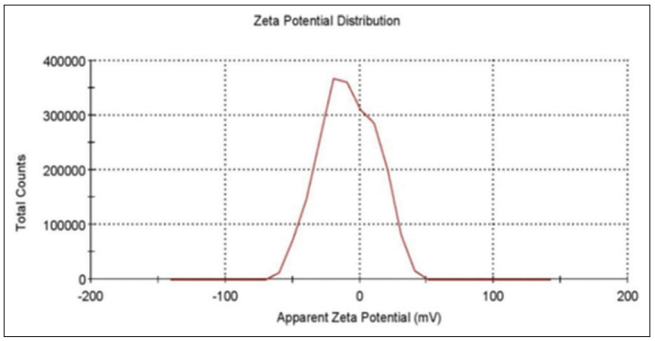

Figure 3: Zeta potential image of formulated nanoemulsion

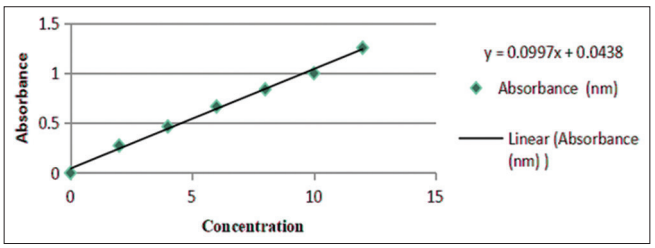

Figure 4: Calibration curve of formulated nanoemulsion

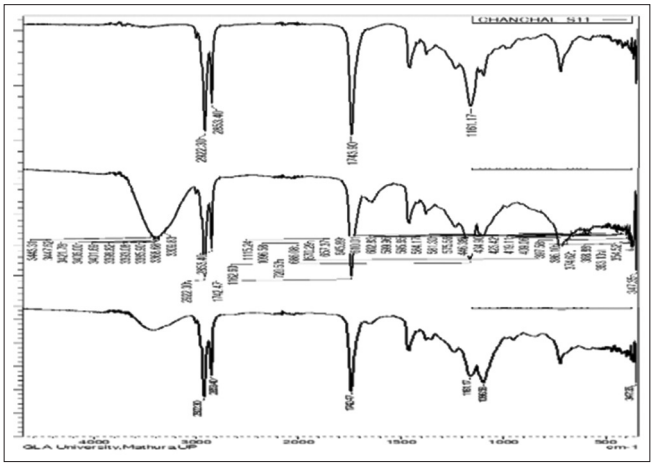

Figure 5: Comparative infrared radiation spectra of sabinene, nanoemulsion formulation, and physical mixture of formulation

Table 5: Formulations of nanoemulsion

S. No.	Ingredients	B1	B2	B3	B4	B5	B6
1	Nirgundi Oil	13 mL	13 mL	13 mL	13 mL	13 mL	13 mL
2	Tween-80	28.5 mL	30.5 mL	32.5 mL	34.5 mL	36.5 mL	38.5 mL
3	Span 20	28.5 mL	30.5 mL	32.5 mL	34.5 mL	36.5 mL	38.5 mL
4	Distilled Water	30 mL	26 mL	22 mL	18 mL	14 mL	10 mL
	Total Vol.	100 mL	100 mL	100 mL	100 mL	100 mL	100 mL

Table 6: Droplet size, polydispersity index, zeta potential, and refractive index of each formulation

Formulation code	Droplet size[#] (nm)	PDI[#]	Zeta potential[#]	Refractive index[#]
B1	98.1±0.16	0.481±0.19	−0.212±0.01	1.465±0.08
B2	102.9±0.23	0.823±0.27	−0.187±0.01	1.485±0.08
B3	88.7±0.08	0.919±0.37	−0.249±0.02	1.462±0.99
B4	113.0±0.09	1.081±0.09	−0.187±0.04	1.458±0.97
B5	99.8±0.42	0.613±0.87	−0.173±0.02	1.454±0.09
B6	101.8±0.17	0.799±0.81	−0.177±0.03	1.464±0.89

[#]*n*=3 ± S.D.; PDI: Polydispersity index

Table 7: Viscosity of various batches of formulated nano-emulsions at different RPM

Speed (RPM)	Viscosity of Batches[#] (cp)					
	B1	B2	B3	B4	B5	B6
0	0	0	0	0	0	0
10	172.5±0.42	169.0±0.54	149.6±0.65	148.0±0.41	123.4±0.21	116.2±0.41
20	167.6±0.52	141.9±0.87	133.4±0.87	123.5±0.44	111.9±0.98	108.0±0.38
40	141.8±0.31	138.4±0.75	125.3±0.31	118.4±0.92	104.0±0.71	92.7±0.81
50	132.0±0.67	121.2±0.23	115.4±0.82	109.5±091	99.4±0.23	94.2±0.97

[#]*n*=3 ± S.D.; cp: Centipoise

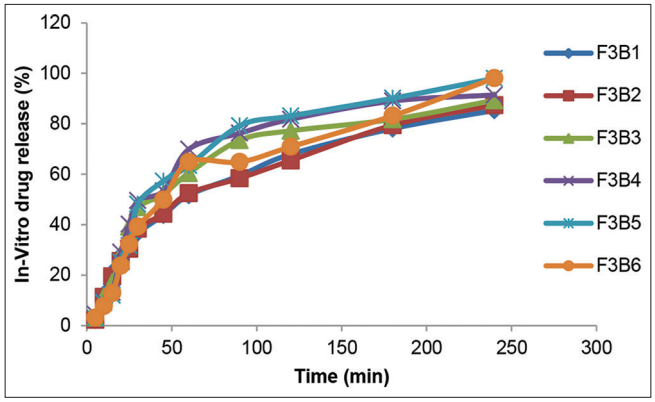

Figure 6: *In vitro* drug release study of various batches of nanoemulsion formulation

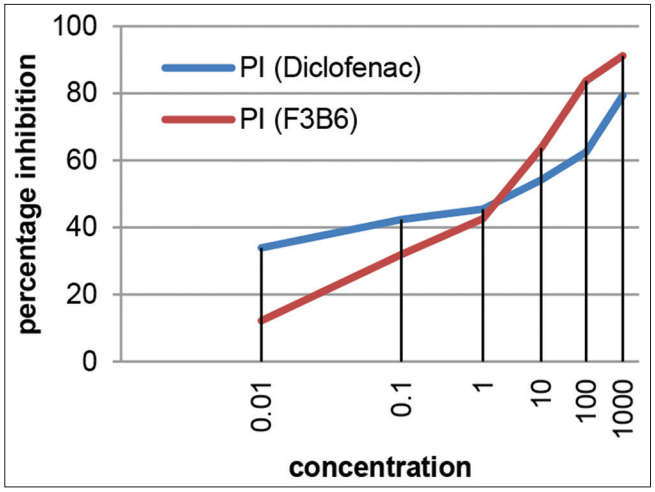

Figure 7: Comparative percent inhibition of reference drug solution and test formulation

pH measurement

The findings of pH study are 4.5, 4.5, 4.7, 4.3, 4.4, and 4.6, respectively, for batches B1 to B6, which represent that the pH of each batch is closely relevant to skin epithelium pH, making it suitable for topical application and will not cause any skin irritation during *in vivo* administration.

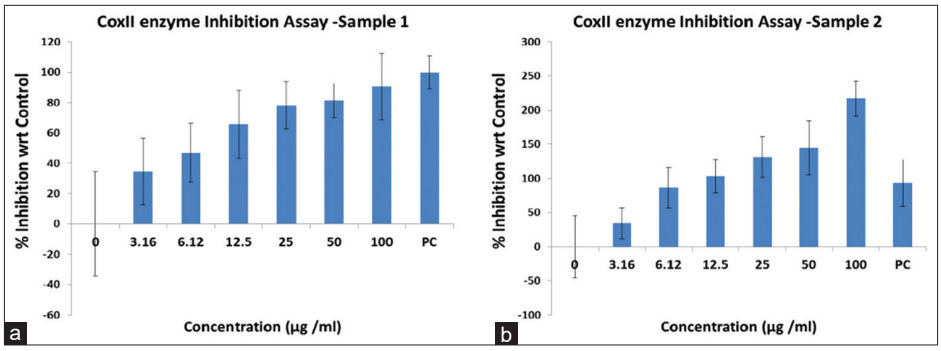

Figure 8: (a and b) Comparative % inhibition control of marker (sabinene) B6 nanoemulsion formulation

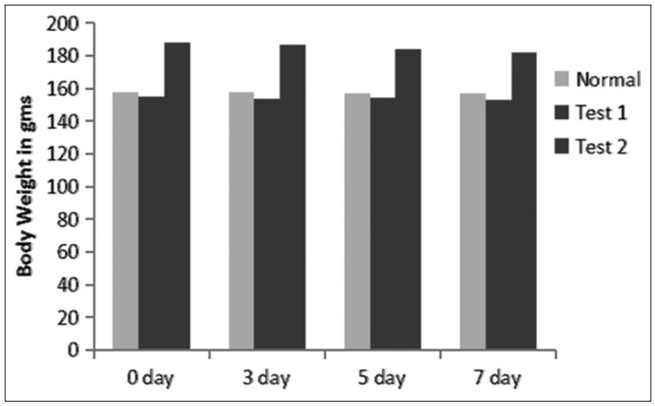

Figure 9: Assessment of the body weight of grouped animals

Viscosity measurement

The findings of viscosity studies are given in Table 7.

Preparation of calibration curve

As seen in Figure 4, a calibration curve was created by measuring the absorbance of dilutions.

FTIR: Drug excipient compatibility study

The IR bands showed no incompatibility between the drug and excipients. The bands of IR were obtained in various regions, such as the sharp bends obtained in the print region and another band in the unsaturated region (2000–2400 cm^{-1}) (Figure 5).

DEE and DLE

Drug entrapment and loading efficiency were measured, and the findings are shown in Table 8.

Thermodynamic stability study

All nanoemulsion formulations were stable at the heating-cooling cycle, and no phase separation was observed during centrifugation (Table 9).

In vitro drug permeation study

The amount of drug permeated from the formulation was higher in B6, 98.01±0.42%, compared to the other formulations B1, B2, B3, B4, and B5, as shown in Figure 6.

Table 8: DEE and DLE of all batches of nanoemulsion formulation

Batch	DEE# (%)	DLE# (%)
B1	94.231±0.10	12.232±0.09
B2	92.849±0.09	12.344±0.08
B3	95.291±0.09	12.139±0.08
B4	95.121±0.08	11.889±0.09
B5	94.231±0.09	11.989±0.12
B6	96.920±0.10	12.975±0.10

#*n*=3 ± S.D

Table 9: Stability status of the heating-cooling cycle (4–45°C) of various batches of formulation 3

Formulation	Heating cooling cycle	Stability status
B1	Phases were not separated	Steady formulation
B2	Phases were not separated	Steady formulation
B3	Phases were not separated	Steady formulation
B4	Phases were not separated	Steady formulation
B5	Phases were not separated	Steady formulation
B6	Phases were not separated	Steady formulation

Selection of best formulation

All the batches of prepared nanoemulsion were evaluated successfully, and all the parameters were found satisfactory and passed the criteria of good nanoemulsion formulation.

Because all other parameters are close to each other, an *in vitro* drug release study found that B6 was more efficacious than all other batches.

In vitro anti-inflammatory activity

- Egg albumin denaturation method
- Cox II enzyme inhibition method

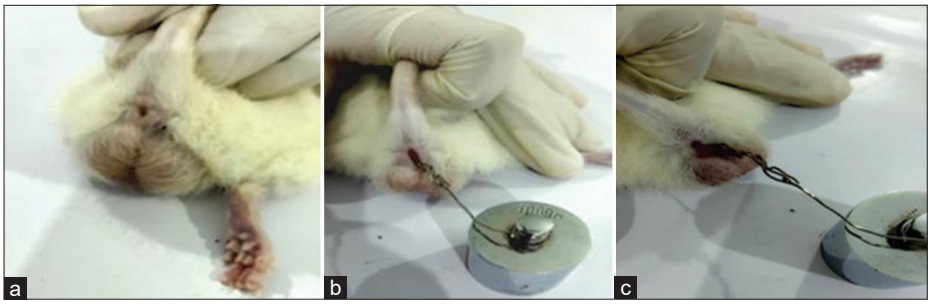

Figure 10: (a-c) Fissure invasion in Group I (Normal), Group II animal (Test I), and Group III animal (Test II)

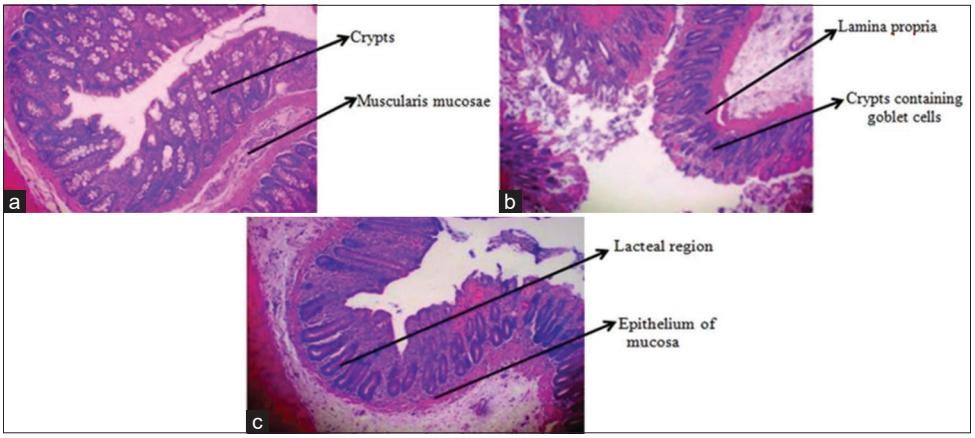

Figure 11: (a-c) Comparative histology of normal group animal anas, Group II animal anas (Test I) treated with marker formulation and Group III animal anas (Test II) treated with marker formulation

Table 10: IC_{50} value of standard and test formulation

Sample code	IC_{50} value
Sample 1 (Sabinene)	6.594 µg/mL
Sample 2 (B6)	3.735 µg/mL

Egg albumin denaturation method

Percentage inhibition of reference drug solution (diclofenac)

Percent inhibition of reference drug, i.e., diclofenac, is shown in Figure 7.

Percentage inhibition of test formulation (B6)

The percent inhibition of the best-selected batch formulated, B6, among prepared nanoemulsions, and Figure 7 shows the comparative percent inhibition.

Cox II enzyme inhibition method

The half maximum inhibitory concentration of marker compound, i.e., sabinene and test formulation, i.e., B6 batch of nanoemulsion is shown here in Table 10 and Figure 8a and b.

In vivo anal fissure healing activity

Anal fissure invasion, groups of animals, and anal fissure healing activity

The body weight of the diseased group animals (test 1: 153±3.244 and test 2: 182±8.888 cm at 7 days) did not significantly alter from that of the control group animals (157.3±7.010 cm) during the whole model creation and standardization process, as seen in Figure 9.

Gross evaluation revealed that the 100 g weight caused a distinct linear rip, slit, or abrasion in the rectal region, as seen in Figure 10a-c. The weight hanging on the wire also indicates induction of the fissure with injury.

Histological examination

Histological examination of anal fissures treated successfully shows notable improvements in tissue architecture compared to untreated fissures as shown in the Figure 11a-c. In treated samples classified as normal, the squamous epithelium appears intact, with a restoration of the normal epithelial layer and absence of necrosis. The inflammatory infiltrate is significantly reduced, indicating a resolution of the acute inflammatory response. Fibrosis may still be present but is less pronounced, suggesting improved healing dynamics. Vascular structures return to a more normal state, with reduced congestion. Furthermore, any changes in the anal sphincter muscle, such as atrophy or degeneration, tend to reverse, reflecting the restoration of normal function. Overall, these histological findings underscore the efficacy of appropriate treatment in promoting healing and restoring the structural integrity of the anal canal.

CONCLUSION

Six batches of nanoemulsion of Nirgundi oil were prepared using Tween-80 and Span 20 polymers in different concentrations on behalf of the prepared phase diagram and evaluated. The best formulation selected was B6 because of its release profile from the formulation. The selected formulation was undergone *in vitro* anti-inflammatory activity and *in vivo* anal fissure healing activity to ensure its therapeutic effect and efficacy of drug formulation in anal fissure. Two types of *in vitro* anti-inflammatory activity were performed with the formulation, i.e., egg albumin denaturation method and COX-II enzyme inhibition. In the egg albumin denaturation methods, the anti-inflammatory activity of the formulation was compared with the marketed drug, i.e., diclofenac, and it was found that the formulation showed more significant action than diclofenac. In the COX-II enzyme inhibition, the anti-inflammatory activity was compared with the marketed drug celecoxib and the pure marker compound of Nirgundi oil (sabinene). The findings assure its significant anti-inflammatory activity. In the anal fissure healing activity, three groups of six male Wistar rats were taken. A nichrome wire (24 SWG) was used to produce an anal fissure in two groups, and one group remained uninvaded. The two groups were treated with the marker formulation and prepared formulation. The histological examination results assured more efficient healing of fissures in the prepared formulation group than marker formulation.

REFERENCES

1. Page MJ, McKenzie JE, Bossuyt PM, Boutron I, Hoffmann TC, *et al.* The PRISMA 2020 statement: An updated guideline for reporting systematic reviews. Int J Surg 2021;88:105906.
2. Youssef T, Youssef M, Thabet W, Lotfy A, Shaat R, Abd-Elrazek E, *et al.* Randomized clinical trial of transcutaneous electrical posterior tibial nerve stimulation versus lateral internal sphincterotomy for treatment of chronic anal fissure. Int J Surg 2015;22:143-8.
3. McCallion K, Gardiner KR. Progress in the understanding and treatment of chronic anal fissure. Postgrad Med J 2001;77:753-8.
4. Nizam R, Ansari MS. Effect of aelwa (*Aloe barbadensis* Mill.) in fissure in ano: A prospective study. Adv Integr Med 2022;9:44-52.
5. Augustinsson LE, Bohlin P, Bundsen P, Carlsson CA, Forssman L, Sjöberg P, *et al*. Pain relief during delivery by transcutaneous electrical nerve stimulation. Pain 1977;4:59-65.
6. Menees S, Chey WD. Fecal incontinence: Pathogenesis, diagnosis, and updated treatment strategies. Gastroenterol Clin North Am 2022;51:71-91.
7. Patkova B, Wester T. Anal fissure in children. Eur J Pediatr Surg 2020;5:391-4.
8. Salem AE, Mohamed EA, Elghadban HM, Abdelghani GM. Potential combination topical therapy of anal fissure: Development, evaluation, and clinical study. Drug Deliv 2018;25:1672-82.
9. Ayduz S, Al-Tabari AI. Firdaws al-hikma (Paradise of Wisdom). Berlin-Charlottenburg: Gesellschaft Mit Beschränkter Haftung; 1928. p. 18.
10. Acheson AG, Scholefield JH. Management of hemorrhoids. BMJ 2008;336:380-3.
11. Dhiman S, Nadda RK, Bhardwaj P. Medicinal herbs from Western Himalayas for hemorrhoids treatment: A review correlating traditional knowledge with modern therapeutics. Pharmacol Res Mod Chin Med 2023;9:100334.
12. Vidyarthi S, Samant SS, Sharma P. Traditional and indigenous uses of medicinal plants by local residents in Himachal Pradesh, North Western Himalaya. India Int J Biodivers Sci Ecosyst Serv Manage 2013;9:185-200.
13. Issa M, Chandel S, Singh HP, Batish DR, Kohli RK, Yadav SS, *et al.* Appraisal of phytotoxic, cytotoxic and genotoxic potential of essential oil of a medicinal plant *Vitex negundo*. Ind Crops Prod 2020;145:112083.
14. Kulkarni RR, Virkar AD, D'mello P. Antioxidant and antiinflammatory activity of *Vitex negundo*. Indian J Pharm Sci 2008;70:838-40.
15. Telang RS, Chatterjee S, Varshneya C. Studies on analgesic and anti-inflammatory activities of *Vitex negundo* linn. Indian J Pharmacol 1999;31:363-6.
16. Sivapalan S, Dharmalingam S, Ashokkumar V, Venkatesan V, Angappan M. Evaluation of the anti-inflammatory and antioxidant properties and isolation and characterization of a new bioactive compound, 3,4,9-trimethyl-7-propyldecanoic acid from *Vitex negundo*. J Ethnopharmacol 2024;319:117314.
17. Prasanna Raja P, Sivakumar V, Riyazullah MS. Antidiabetic potential of aqueous and ethanol leaf extracts of *Vitex negundo*. Int J Pharm Phytochem Res 2012;4:38-40.
18. Harwansh RK, Deshmukh R, Rahman A. Nanoemulsion: Promising nanocarrier system for delivery of herbal bioactives. J Drug Del Sci Tech 2019;51:224-33.
19. Sneha K, Kumar A. Nanoemulsions: Techniques for the preparation and the recent advances in their food applications. Innov Food Sci Emerg Technol 2022;76:102914.
20. Vater C, Bosch L, Mitter A, Göls T, Seiser S, Heiss E, *et al.* Lecithin-based nanoemulsions of traditional herbal wound healing agents and their effect on human skin cells. Eur J Pharm Biopharm 2022;170:1-9.
21. Artiga-Artigas M, Guerra-Rosas MI, Morales-Castro J, Salvia-Trujillo L, Martín-Belloso O. Influence of essential oils and pectin on nanoemulsion formulation: A ternary phase experimental approach. Food Hydrocoll 2018;81:209-19.
22. Mazonde P, Khamanga SM, Walker RB. Design, optimization, manufacture and characterization of efavirenz-loaded flaxseed oil nanoemulsions. Pharmaceutics 2020;12:797.

23. Barrios CA, Mirea T, Represa MH. A self-referenced refractive index sensor based on gold nanoislands. Sensors (Basel) 2023;23:66-77.
24. Hussain A, Afzal O, Altamimi AS, Ali R. Application of green nanoemulsion to treat contaminated water (bulk aqueous solution) with azithromycin. Environ Sci Pollut Res Int 2021;28:61696-706.
25. El-Leithy ES, Makky AM, Khattab AM, Hussein DG. Optimization of nutraceutical coenzyme Q10 nanoemulsion with improved skin permeability and anti-wrinkle efficiency. Drug Dev Ind Pharm 2018;44:316-28.
26. Arianto A, Cindy C. Preparation and evaluation of sunflower oil nanoemulsion as a sunscreen. Open Access Maced J Med Sci 2019;7:3757-61.
27. Shah D, Guo Y, Ban I, Shao J. Intranasal delivery of insulin by self-emulsified nanoemulsion system: *In vitro* and *in vivo* studies. Int J Pharm 2022;616:121565.
28. Liang CX, Qi DL, Zhang LN, Lu P, Li ZD. Preparation and evaluation of a water-in-oil nanoemulsion drug delivery system loaded with salidroside. Chin J Nat Med 2021;19:231-40.
29. Wang Y, Geng M, Zhang XX, Yan M, Sun L, Zhao Q. Preparation of lutein nanoemulsion by ultrasonic homogenization method: Stability and *in vitro* anti-inflammatory activity. Algal Res 2023;73:103154.
30. Hsieh IT, Chou TH, Chang JS. Development, characterization, and *in vitro* biocompatibility of evening primrose oil nanoemulsions using ultrasonic nano-emulsification technology. J Taiwan Inst Chem Eng 2023;160:105311.
31. Joarddar P, Saha P, Sarkar S, Jana AD. Water assisted self-assembly of cu(II)(pyridine-3-carboxylate)$_2$(H2O)$_4$ coordination complexes and pH dependent growth of microtubes around the crystals - X-ray crystallographic, FESEM, spectroscopic and DFT studies. J Mol Struct 2024;1301:137310.
32. Liu A, Liu S, Liu Y, Liu B, Liu T. Characterizing mechanical heterogeneity of coal at nano-to-micro scale using combined nanoindentation and FESEM-EDS. Int J Coal Geol 2022;261:104081.
33. Laxmi M, Bhardwaj A, Mehta S, Mehta A. Development and characterization of nanoemulsion as carrier for the enhancement of bioavailability of artemether. Artif Cells Nanomed Biotechnol 2015;43:334-44.
34. Lu GW, Gao P. Emulsions and microemulsions for topical and transdermal drug delivery. Kulkarni VS, editor. In: Personal Care Cosmetic Technology. Handbook of Non-Invasive Drug Delivery Systems. Ch. 3. New York: William Andrew Publishing; 2010. p. 59-94.
35. Kurpiers M, Wolf JD, Steinbring C, Zaichik S, Bernkop-Schnürch A. Zeta potential changing nanoemulsions based on phosphate moiety cleavage of a PEGylated surfactant. J Mol Liq 2020;316:113868.
36. Hua S. Physiological and pharmaceutical considerations for rectal drug formulations. Front Pharmacol 2019;10:1196.
37. Webster D. PH - principles and measurement. In: Caballero B, editor. Encyclopedia of Food Sciences and Nutrition. 2nd ed. United States: Academic Press; 2003. p. 4501-7.
38. Alliod O, Messager L, Fessi H, Dupin D, Charcosset C. Influence of viscosity for oil-in-water and water-in-oil nanoemulsions production by SPG premix membrane emulsification. Chem Eng Res Des 2019;142:87-99.
39. JoVE Science Education Database. Analytical chemistry. In: Calibration Curves. Cambridge, MA: JoVE; 2024.
40. Chander S, Komal R, Nikita Y, Nidhi B, Yogesh V, Shalini K, *et al*. A review: Drug excipient iincompatiblity by ftir spectroscopy. Curr Pharm Anal 2023;19:371-8.
41. Song X, Zhao Y, Hou S, Xu F, Zhao R, He J, *et al*. Dual agents loaded PLGA nanoparticles: Systematic study of particle size and drug entrapment efficiency. Eur J Pharm Biopharm 2008;69:445-53.
42. Reddy GS, Thakur A. Drug entrapment efficiency of silver nanocomposite hydrogel. Mater Sci Eng 2019;577:012176.
43. Ali MS, Alam MS, Alam N, Siddiqui MR. Preparation, characterization and stability study of dutasteride loaded nanoemulsion for treatment of benign prostatic hypertrophy. Iran J Pharm Res 2014;13:1125-40.
44. Kumar N, Mandal A. Thermodynamic and physicochemical properties evaluation for formation and characterization of oil-in-water nanoemulsion. J Mol Liq 2018;266:147-59.
45. Kim BS, Won M, Lee KM, Kim CS. *In vitro* permeation studies of nanoemulsions containing ketoprofen as a model drug. Drug Deliv 2008;15:465-9.
46. Franz TJ. Percutaneous absorption on the relevance of *in vitro* data. J Invest Dermatol 1975;64:190-5.
47. Shakeel F, Baboota S, Ahuja A, Ali J, Aqil M, Shafiq S. Nanoemulsions as vehicles for transdermal delivery of aceclofenac. AAPS Pharm Sci Tech 2007;8:E104.
48. Chaiya P, Senarat S, Phaechamud T, Narakornwit W. *In vitro* anti-inflammatory activity using thermally inhibiting protein denaturation of egg albumin and antimicrobial activities of some organic solvents. Mater Today Proc 2022;65:2290-5.
49. Madhuranga HD, Samarakoon DN. *In vitro* anti-inflammatory egg albumin denaturation assay: An enhanced approach. J Nat Ayurvedic Med 2023;7:000411.
50. Dharmadeva S, Galgamuwa LS, Prasadinie C, Kumarasinghe N. *In vitro* anti-inflammatory activity of *Ficus racemosa* L. Bark using albumin denaturation method. Ayu 2018;39:239-42.
51. Chandra S, Chatterjee P, Dey P, Bhattacharya S. Evaluation of *in vitro* anti-inflammatory activity of coffee against the denaturation of protein. Asian Pac J Trop Biomed 2012;2:S178-80.
52. Zarghi A, Arfaei S. Selective COX-2 inhibitors: A review of their structure-activity relationships. Iran J Pharm Res 2011;10:655-83.
53. Landa P, Kokoska L, Pribylova M, Vanek T, Marsik P. *In vitro* anti-inflammatory activity of carvacrol: Inhibitory effect on COX-2 catalyzed prostaglandin E(2)

biosynthesis. Arch Pharm Res 2009;32:75-8.
54. Srivastava JK, Pandey M, Gupta S. Chamomile, a novel and selective COX-2 inhibitor with anti-inflammatory activity. Life Sci 2009;85:663-9.
55. Rao P, Knaus EE. Evolution of nonsteroidal anti-inflammatory drugs (NSAIDs): Cyclooxygenase (COX) inhibition and beyond. J Pharm Pharm Sci 2008;11:81s-110.
56. Ju Z, Li M, Xu J, Howell DC, Li Z, Chen FE. Recent development on COX-2 inhibitors as promising anti-inflammatory agents: The past 10 years. Acta Pharm Sin B 2022;12:2790-807.
57. Chahal S, Rani P, Kiran, Sindhu J, Joshi G, Ganesan A, *et al.* Design and development of COX-II inhibitors: Current scenario and future perspective. ACS Omega 2023;8:17446-98.
58. Walker MC, Gierse JK. *In vitro* assays for cyclooxygenase activity and inhibitor characterization. Methods Mol Biol 2010;644:131-44.
59. Famaey J. *In vitro* and *in vivo* pharmacological evidence of selective cyclooxygenase-2 inhibition by nimesulide: An overview. Inflamm Res 1997;46:437-46.

Source of Support: Nil. **Conflicts of Interest:** None declared.